Superconductivity above 30 K in $[(Bi_{1-x}Mo_x)_{0.33}Cu_{0.67}]Sr_2YCu_2O_y$: Appearance of superconductivity by transfer of holes from a block layer to a CuO_2 layer

Shiro Kambe and Eiji Sato
Graduate School of Engineering, Yamagata University, 4-3-16, Jonan, Yonezawa, Yamagata 992, Japan

Takahiro Akao, Shigetoshi Ohshima, and Katsuro Okuyama
Faculty of Engineering, Yamagata University, 4-3-16, Jonan, Yonezawa, Yomagata 992, Japan

Rika Sekine
Department of Chemistry, Shizuoka University, 836, Ohya, Shizuoka 442, Japan
(Received 26 May 1998; revised manuscript received 17 February 1999)

Attention has been paid to a $(Bi_{0.33}Cu_{0.67})Sr_2YCu_2O_y$ compound for its uncertain superconductivity in spite of having a large Cu valence. By conducting combined experiments of iodometry, and chlorinemetry, Hall voltage measurement, Rietveld analysis, and a Discrete vibrational (DV)-$X\alpha$ calculation for $(Bi_{0.33}Cu_{0.67})Sr_2YCu_2O_y$, evidence of localization of holes in a $(Bi_{0.33}Cu_{0.67})O_y$ block layer was found. Those experiments suggest that about 90% of holes estimated from the Mott-Hubbard theory are localized. DV-$X\alpha$ calculation revealed that the localized holes in $(Bi_{0.33}Cu_{0.67})Sr_2YCu_2O_y$ are not located at the apical or planar oxygen of a CuO_2 layer but in the block layer. In order to transfer the localized holes from the block layer to the CuO_2 layer, substitution of Mo for Bi was performed, resulting in an increase of the itinerant holes from 10 to 60 %. A bond valence sum calculation also suggested the transfer of holes from the block layer to the CuO_2 layer with changes in occupancies of the oxygen sites in the block layer. Eventually, in a range of $x \geqslant 0.55$, it showed superconductivity above 30 K. We also discuss the origin of nonsuperconductivity of cuprates with a high Cu valence. [S0163-1829(99)04025-4]

I. INTRODUCTION

Attention has been paid to (Bi,Cu)-1212 phase with a composition of $(Bi_{1-x}Cu_x)Sr_2YCu_2O_y$ for its uncertain superconductivity in spite of having a Cu valence large enough to induce superconductivity. The (Bi,Cu)-1212 phase was first prepared by Ehmann *et al.*[1] They reported that the compound is superconducting below a temperature of 68 K with a nominal composition of $(Bi_{0.5}Cu_{0.5})Sr_2Y_{0.8}Cu_{2.2}O_{0.95}$. Unfortunately, it contains impurities including a Bi-2212 phase. Afterwards Wang *et al.*[2] reported that the superconductivity observed by Ehmann *et al.* is not due to the (Bi,Cu)-1212 phase but due to the impurity. It was also reported that by sintering the powerful with a nominal composition of $(Bi_{0.3}Cu_{0.7})Sr_2YCu_2O_y$, a nearly single phase of the (Bi, Cu)-1212 sample[2,3] was prepared and that annealing the sample in oxygen with a pressure of 400 atm induced superconductivity below a temperature of 20 K.[2] However, according to the X-ray diffraction (XRI) data observed by them, impurity peaks still remained in the prepared sample. The superconducting volume fraction estimated from a Meissner signal at 5 K was as small as 1.5%. Therefore, there is the possibility that superconductivity comes from such impurities, not from the (Bi,Cu)-1212 phase.

In a previous paper,[4] we reported the successful preparation of the $(Bi_{1-x}Cu_x)Sr_2YCu_2O_y$ phase. In order to obtain the pure single phase sample, controls of nominal composition and sintering atmosphere were required. We also reported that a single phase of (Bi,Cu)-1212 is not superconducting but semiconducting in spite of having a high Cu valence larger than 2.1. Now, it is interesting to examine the origin of the nonsuperconductivity of the (Bi,Cu)-1212 phase.

In this paper, we first focused our study on the origin of nonsuperconductivity of $(Bi_{1-x}Cu_x)Sr_2YCu_2O_y$. We confirmed the preparing condition of $(Bi_{1-x}Cu_x)Sr_2YCu_2O_y$, refined its crystal structure by Rietveld analysis, measured its hole density, and calculated electronic states of the CuO_2 layer by DV-$X\alpha$ calculation, revealing that 90% of the holes are localized in the block layer.

Secondly, based on these results, we tried to make $(Bi_{1-x}Cu_x)Sr_2YCu_2O_y$ superconducting by substitution of Bi for the other transition metals. We found that Mo is the most helpful element for occurrence of superconductivity. A solid solution $[(Bi_{1-x}Mo_x)_{0.33}Cu_{0.67}]Sr_2YCu_2O_y$ was prepared for $0 \leqslant x \leqslant 1.0$. From the resistivity measurements as a function of temperature, superconductivity was shown in the region of $0.55 \leqslant x \leqslant 1.0$. Mo substitution increased the itinerant holes from 10 to 60 %, resulting in superconductivity above 37 K.

Finally, we discuss the origin of nonsuperconductivity of cuprates with a Cu valence larger than 2.1. Part of the results have already been published in Refs. 4–6.

II. EXPERIMENT

Samples of $(Bi_{1-x}Cu_x)Sr_2YCu_2O_y$ $(0.5 \leqslant x \leqslant 0.8)$ and $[(Bi_{1-x}Mo_x)_{0.33}Cu_{0.67}]Sr_2YCu_2O_y$ $(0.0 \leqslant x \leqslant 1.0)$ were prepared by a conventional mixing method.[4] As shown in Fig. 1, a pellet was prepared by mixing Bi_2O_3, $SrCO_3$, Y_2O_3, CuO, and MoO_3 in an agate mortar, calcining at 850–900 °C in air for 5–10 h, grinding it in the mortar again, pressing it into a pellet, and then sintering at 980 °C in air for 20–60 h. After sintering, the pellet was quenched to a room temperature on a metal plate or cooled slowly in a furnace. After grinding it to powder, a single phase of the (Bi,Cu)-1212 powder was

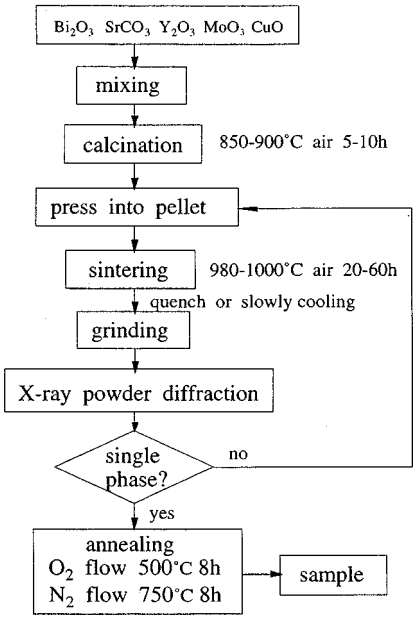

FIG. 1. Preparation of $(Bi_{0.33}Cu_{0.67})Sr_2YCu_2O_y$ and $[(Bi_{1-x}Mo_x)_{0.33}Cu_{0.67}]Sr_2YCu_2O_y$ compounds.

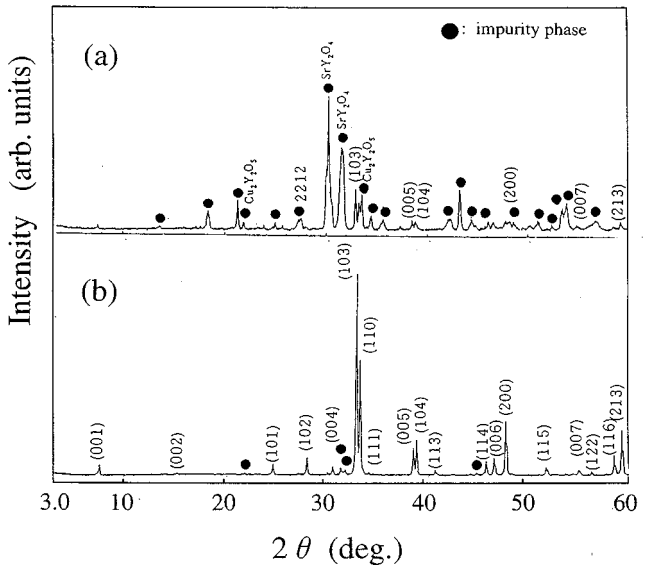

FIG. 2. XRD patterns of (Bi,Cu)-1212 samples synthesized under (a) slowly cooled and (b) quenched condition. Quenching drastically decreases the impurity phase.

ascertained by an XRD method. In order to obtain an optimum hole concentration, oxygen content was varied by annealing in an atmosphere of N_2 or O_2.

The cation ratio of the prepared sample determined by inductively coupled plasma (ICP) atomic emission spectroscopy measurement was consistent with the nominal ratio within 5%. Its structural parameters were determined by a Rietveld analysis (RIETAN).[7] Errors of oxygen occupancy O(1)–O(4) were estimated from the standard deviation. We assumed that the blocking layer has two oxygen sites O(3) and O(4) and refined occupancies of the O(3) and O(4) sites by the Rietveld analysis with fixing total oxygen content.

The total oxygen content was determined by an iodometric method. Bi and Cu valences were determined separately by combining the iodometric and the chlorine production method.[8] Here, the valence of Mo is assumed to be Mo(VI), respectively. If a Mo(II or V) is to exist, the Cu valence should be corrected. According to the Mott-Hubbard theory, by subtracting 2 from the Cu valence, a number of holes per Cu v was calculated.

Since the v represents an average number of holes per Cu, if the valence of Cu in the (Bi,Cu,O) layer is different from that in the CuO_2 layer, the number of holes in the (Bi,Cu,O) layer or CuO_2 layer should be corrected. Nevertheless, the whole number of holes per unit cell is not changed, even though the Cu in the (Bi,Cu,O) layer has a different valence than that in the CuO_2 layer. Therefore, we can estimate the whole number of holes v in a unit cell correctly from the Cu valence.

Resistivity-temperature curves ($10\,K \leqslant T \leqslant 300\,K$) were measured by a conventional four-probe method. The superconducting properties were also determined by measuring the temperature dependence of ac magnetic susceptibility, by the field cooling method (Meissner effect). The magnetic field of 2 Oe with a frequency of 313 Hz was applied to the reground sample.

For the Hall voltage measurement, low resistance contacts to the sample (about 8 mm×5 mm×1 mm in size) were made by using conducting silver paste. A four-wire ac resistance bridge (LR-400, Linear Research, Inc.) was used for measuring Hall voltage across the Hall terminals. A current of 1–10 mA was flowed through the sample and the applied magnetic field strength was fixed at ±1.5 T.

From the Hall coefficient R_H, hole density n_H was induced from the following equation:

$$n_H = \frac{1}{qR_H}, \tag{1}$$

where q represents the elementary electric charge. Assuming that the holes are located in the CuO_2 layer, the number of holes per Cu p is calculated by

$$p = \frac{n_H V}{s}, \tag{2}$$

where V and s represent the unit cell volume and the number of Cu in the unit cell, respectively. The ratio of delocalized holes r was estimated by the equation

$$r = \frac{p}{v}, \tag{3}$$

where v represents the number of holes per Cu estimated from the Cu valence by the Mott-Hubbard theory and is determined by the following equation:

$$v = (\text{Cu valence}) - 2. \tag{4}$$

The numerical computation was carried out by a DV-$X\alpha$ method.[9] The exchange parameter a is fixed at 0.7 through all calculations. The numerical atomic orbitals of $1s$-$4p$ for Cu and of $1s$-$2p$ for O are utilized for basis functions of the linear combination of atomic orbitals (LCAO).

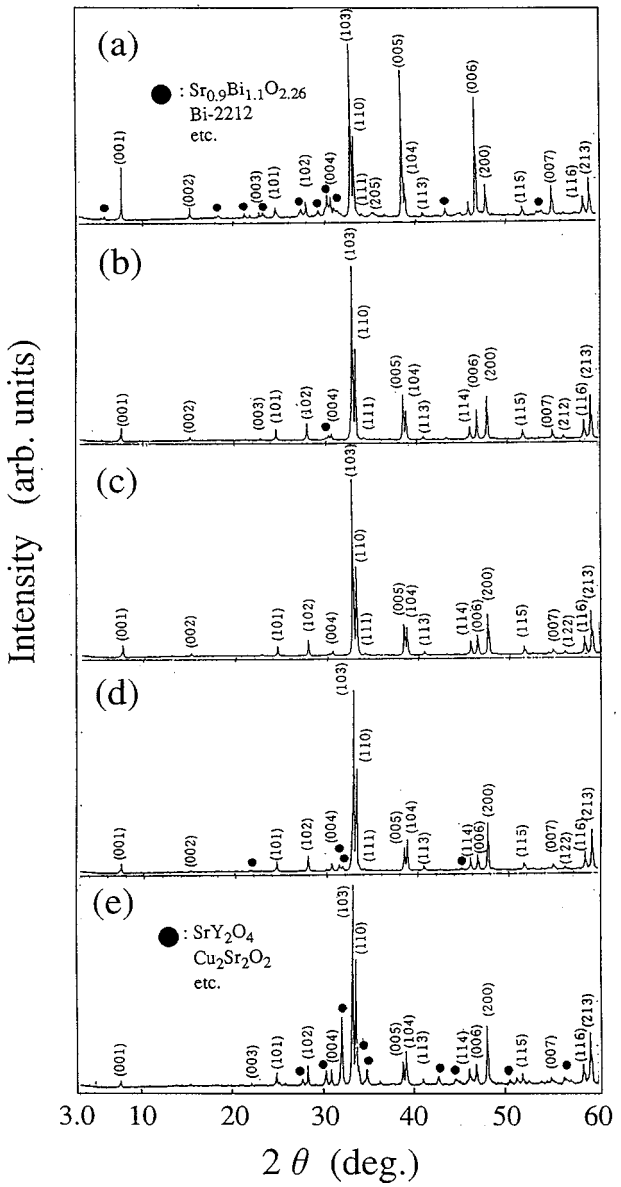

FIG. 3. XRD patterns of $(Bi_{1-x}Cu_x)Sr_2YCu_2O_y$, (a) $x=0.50$, (b) $x=0.65$, (c) $x=0.67$, (d) $x=0.70$, and (e) $x=0.80$.

III. RESULTS AND DISCUSSION

A. $(Bi_{1-x}Cu_x)Sr_2YCu_2O_y$ phase

Preparation of $(Bi_{1-x}Cu_x)Sr_2YCu_2O_y$. Figures 2(a) and 2(b) show XRD patterns of (Bi,Cu)-1212 samples synthesized under slowly cooled and quenched conditions, respectively. As shown in Fig. 2, impurity phases such as Bi-2212, $Cu_2Y_2O_5$, and SrY_2O_4 were drastically decreased by the quenching treatment. Therefore, all the samples hereafter were fabricated by the quenching method.

In order to confirm an optimum Bi/Cu ratio, the x value in the $(Bi_{1-x}Cu_x)Sr_2YCu_2O_y$ phase was successively changed between 0.5 and 0.8. Figure 3 shows the change in XRD peaks as a function of x, showing that in a very narrow region around $x=0.67$, a single phase of the (Bi,Cu)-1212 sample was prepared.

For the oxygen-annealed sample of $(Bi_{0.33}Cu_{0.67})Sr_2YCu_2O_y$, Rietveld analysis was carried out. Refined crystallographic data for this sample are displayed in Fig. 4 and Table I. The interatomic distances are listed in Table II. We assumed that the blocking layer has two oxygen sites O(3) and O(4), as shown in Fig. 5. Reliability factor R_{wp} for the model was 5.79%, indicating that this model is an appropriate one. The model is comparable to that proposed by Wang *et al.*,[2] except for its oxygen content. While they fixed its oxygen content to be 7.5, we fixed it to be 6.9 from the result of iodometry. A structural feature of this sample is existence of double CuO_2 planes with an apical oxygen, separated from each other by Y layer. This structure is commonly seen in high-T_c superconductors with T_c values higher than 80 K such as a $YBa_2Cu_3O_7$ superconductor. Therefore, it is expected that the $(Bi_{0.33}Cu_{0.67})Sr_2YCu_2O_{6.9}$ induces superconductivity with a T_c higher than 80 K.

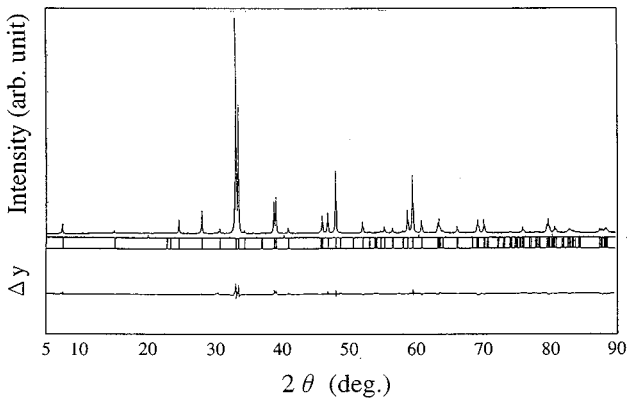

FIG. 4. An XRD pattern of $(Bi_{0.33}Cu_{0.67})Sr_2YCu_2O_y$. The dotted and solid lines represent an observed pattern and that refined by Rietveld analysis, respectively. A pattern at the bottom is difference between the observed and refined intensities.

As shown in Fig. 6, by changing the annealing atmosphere, oxygen content was varied from 6.77 to 6.88 together with a change in the Cu valence from 2.04 to 2.13. A Bi valence against oxygen content y is also displayed in Fig. 6, indicating that an increase in oxygen content did not raise the Bi valence: the Bi valence was about 3.29 for all the samples while the Cu valence was varied between 2.04 and 2.13. From the fact that the Cu valence 2.13 is equal to that of a 60-K-class $YBa_2Cu_3O_{6.76}$ superconductor, we think that the Cu valence 2.13 is large enough to induce superconductivity and that optimization of the Cu valence for occurrence of

TABLE I. Crystallographic data for $(Bi_{0.33}Cu_{0.67})Sr_2YCu_2O_y$. Lattice constants: $a=3.8135(9)$ [Å], $c=11.705(8)$ [Å]. Space Group: Tetragonal $P4/mmm$ (Vol. A, No. 123), $R_{wp}=5.79\%$, $R_P=4.21\%$, $R_E=5.18\%$, $R_I=4.91\%$, $R_F=3.87\%$.

Atom	Site	x	y	z	Occupation	B [Å^2]
Bi	1*a*	0	0	0	0.33	0.5
Cu(1)	1*a*	0	0	0	0.67	0.5
Sr	2*h*	1/2	1/2	0.2035(8)	1	0.5
Y	1*d*	1/2	1/2	1/2	1	0.2
Cu(2)	2*g*	0	0	0.358(4)	1	0.5
O(1)	4*i*	0	1/2	0.376(3)	0.95(3)	0.5
O(2)	2*g*	0	0	0.163(4)	0.94(4)	1.5
O(3)	1*c*	1/2	1/2	0	0.6(1)	1.5
O(4)	2*f*	0	1/2	0	0.2(8)	1

TABLE II. Interatomic distances [Å] for $(Bi_{0.33}Cu_{0.67})Sr_2YCu_2O_{6.79}$.

		Interatomic distance (Å)
[Bi,Cu(1)]	Sr	3.598(8)
	O(2)	1.913(5)
	O(3)	2.696(6)
	O(4)	1.906(8)
Sr	Cu(2)	3.249(0)
	O(1)	2.779(1)
	O(2)	2.737(2)
	O(3)	2.383(2)
	O(4)	3.052(1)
Y	O(1)	2.394(2)
	Cu(2)	3.165(3)
Cu(2)	O(1)	1.918(3)
	O(2)	2.282(3)

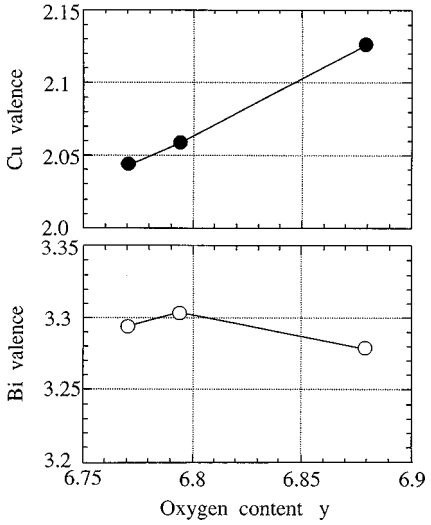

FIG. 6. Cu and Bi valences vs oxygen content (y) for $(Bi_{0.33}Cu_{0.67})Sr_2YCu_2O_y$.

superconductivity is achieved for this sample. In Fig. 7, the dependence of resistivity on temperature is shown. An increase in the oxygen content y from 6.77 to 6.88 led to a drastic decrease in resistivity from 2.06×10^{2} to $1.35\times10^{-1}\,\Omega$ cm at 100 K. However, the sample, whose Cu valence was optimized to be 2.13, was not superconducting but still semiconducting.

According to the Hall effect measurement, the hole density of the oxygen-annealed sample was $3.6\times10^{20}\,cm^{-3}$ at room temperature. This value is much smaller than $3.1\times10^{21}\,cm^{-3}$ for a $YBa_2Cu_3O_{6.76}$ sample.[10] In Fig. 8, the hole density n_H and the ratio of itinerant holes p/v are shown. With an increase in the Cu valence from 2.08 to 2.16, the hole density was increased from 1.0×10^{19} to $3.6\times10^{20}\,cm^{-3}$. These values of hole density measured by the Hall effect measurement are much smaller than those calculated by the Mott-Hubbard model assuming that an increase in the Cu valence from 2.0 to 3.0 dopes one hole to the Cu ion [represented by a broken line in Fig. 8(a)], resulting that the hole density measured by the Hall voltage measurement did not reach the hatched optimum hole density region, necessary for the occurrence of superconductivity. In spite of the optimization of the Cu valence for the (Bi,Cu)-1212 phase, its hole density was extremely small in comparison with the $YBa_2Cu_3O_{6.76}$ superconductor. Therefore, it is revealed that holes induced by the excess oxygen are not doped to the CuO_2 plane sufficiently. While the ratio of itinerant holes p/v in Bi-based superconductors was as large as 100–200 %,[20] the ratio of the N_2-, air-, and O_2-annealed $(Bi_{0.33}Cu_{0.67})Sr_2YCu_2O_y$ specimens was 0.02, 3, and 14 %, respectively [Fig. 8(b)], indicating that the majority of holes are localized somewhere.

The first site where holes may be localized is apical oxygen. The distance between the apical oxygen and the CuO_2 plane of the (Bi,Cu)-1212 phase is about 2.28 Å, which is 0.15 Å shorter than that of the Bi-2212 phase. The extremely short Cu-O(apex) distance may localize holes at the apical

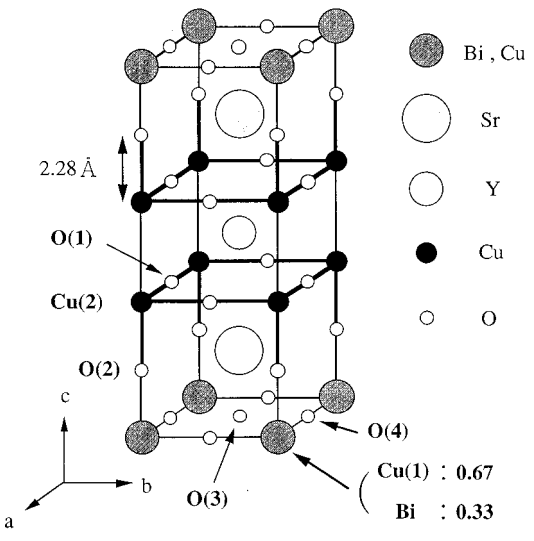

FIG. 5. Crystal structure of the $(Bi_{0.33}Cu_{0.67})Sr_2YCu_2O_y$.

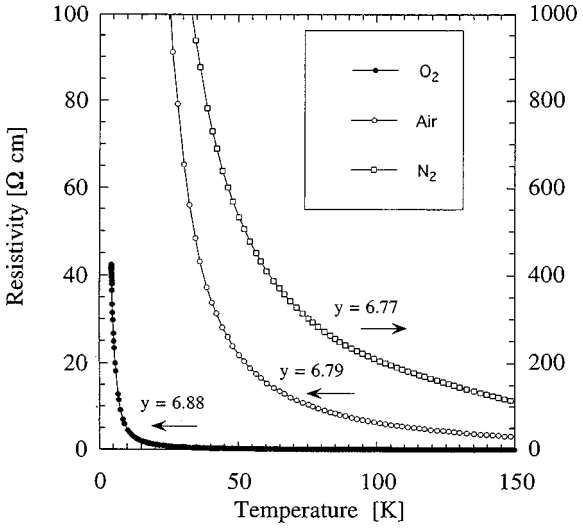

FIG. 7. The dependence of resistivity on the temperature for $(Bi_{0.33}Cu_{0.67})Sr_2YCu_2O_y$. ●, ○, and □ indicate samples annealed in O_2, air, and N_2, respectively.

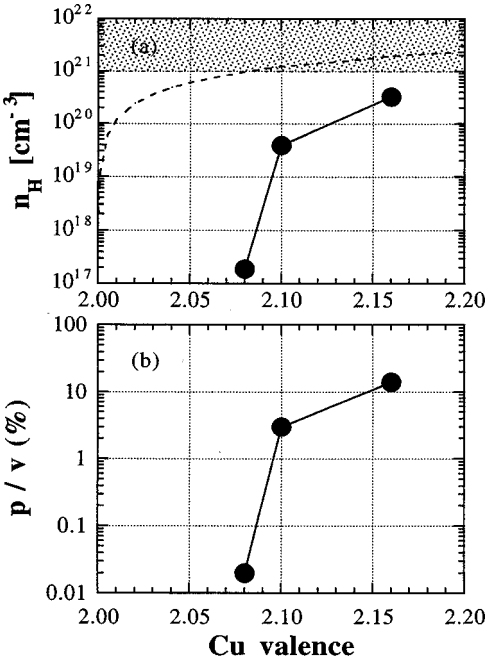

FIG. 8. Hole density (n_h) and ratio of itinerant holes (p/v) against Cu valence.

oxygen and suppress its superconductivity. The second site is in the $(Bi,Cu)O_{1+z}$ layer. We estimated the Cu valence to be 2.13. This is indeed the case if the Cu(1) and the Cu(2) valences are equal. If the valence of the Cu(1) atom in the $(Bi,Cu)O_{1+z}$ plane is larger than the expected one, the hole density in the CuO_2 plane will be smaller than the estimated value 2.13. Furthermore, the Bi valence in the $(Bi,Cu)O_{1+z}$ layer of the (Bi,Cu)-1212 phase is 3.29, which is relatively high compared with 3.03–3.17, those of the Bi-2212 superconductors,[11] suggesting that the holes may be localized in the $(Bi,Cu)O_{1+z}$ layer. In order to elucidate where the holes are localized, electronic states of the CuO_2 layer were calculated by a DV-$X\alpha$ molecular orbital calculation method.

Simulation of electronic structure of $(Bi_{0.33}Cu_{0.67})Sr_2YCu_2O_y$ *by the DV-Xα method.* We believe that the nonsuperconductivity of the $(Bi_{0.33}Cu_{0.67})Sr_2YCu_2O_y$ is strongly correlated with the microstructure of the CuO_2 layer. Consequently, the DV-$X\alpha$ method was applied to a distorted pyramidal CuO_5 cluster in the $(Bi_{0.33}Cu_{0.67})Sr_2YCu_2O_y$. The structure of the CuO_5 cluster is shown in Fig. 9. Three structural parameters used for the CuO_5 cluster are the Cu-O(plane) length, the Cu-O(apex) length, and buckling. The symmetrized orbital of the C_4V group was used. By changing the total electron number in the CuO_5 cluster, the hole density was controlled by changing the number of total electrons in the cluster. We used O_{1s}-O_{2p} and Cu_{1s}-Cu_{4p} orbitals as the ground state function.

In this case, only the pyramidal CuO_5 cluster was considered for the calculation and no external electric field was considered. The electronic states of the CuO_5 cluster in the Bi-2212 and Y-123 superconductors were compared with that of $(Bi_{0.33}Cu_{0.67})Sr_2YCu_2O_y$. In particular, we focused our calculation on the localization of holes at apical oxygen. The structural parameters of the Bi-2212 and Y-123 superconductors were cited from Imai *et al.*[12] and Izumi *et al.*,[13]

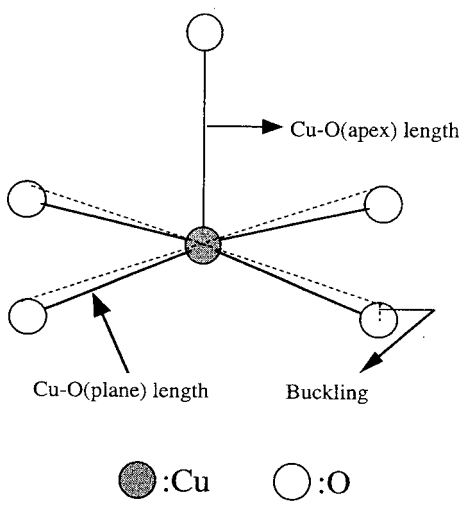

FIG. 9. Structure of the CuO_5 cluster.

respectively. In this calculation, 0.16 of holes were doped into the $(Bi_{0.33}Cu_{0.67})Sr_2YCu_2O_y$, Bi-2212, and Y-123 phases. Thus, the calculation for $(CuO_5)^{-7.84}$ was carried out. All parameters of the CuO_5 cluster used for DV-$X\alpha$ calculation are listed in Table III.

The molecular orbital energy levels near the Fermi level (E_r) calculated by the DV-$X\alpha$ method are shown in Fig. 10. Here, the solid and dashed lines correspond to the occupied and the unoccupied orbitals, respectively. The notations at the right side such as $8A1$, $4E$, etc., denote the irreducible representation of the $C4v$ point group and the sequential number of each irreducible group. The molecular orbital with the same notation is connected by the dashed and dotted lines. First of all, we are aware that the change in the sequence of molecular orbitals for each model is small. This is because the electronic structure is not largely changed by the slight changes in geometry between the models for the (Bi, Cu)-1212, Bi-2201, and Y-123 systems. Especially, the hole doped level is the $5B1$ state for all clusters, which are constituted by the hybridized $Cu3d_{x2-y2}$ and $O2p_{xy}$ orbitals of planar oxygens. Therefore, not only for the Bi-2212 and Y-123 superconductors but for the (Bi,Cu)-1212 phase, a hole located in the CuO_5 cluster is doped to the Cu-O(plane) orbital, resulting in holes that will be contributed to the electric conduction.

The hole distribution on each element was calculated from effective charges obtained by a Mulliken population analysis.[9] Here, the hole number is defined by the subtraction of the formal charge from the effective charge. The hole

TABLE III. Parameters of the CuO_5 cluster used for DV-$X\alpha$ calculation.

Sample	(Bi,Cu)-1212	Bi-2212	Y-123
Cu-O(plane) length (Å)	1.92	1.92	1.94
Cu-O(apex) length (Å)	2.3	2.46	2.26
Buckling (Å)	0.22	0	0.28
Number of holes	0.16	0.16 (0.20)	0.16 (0.20)
Reference	This work	Ref. 12	Ref. 13

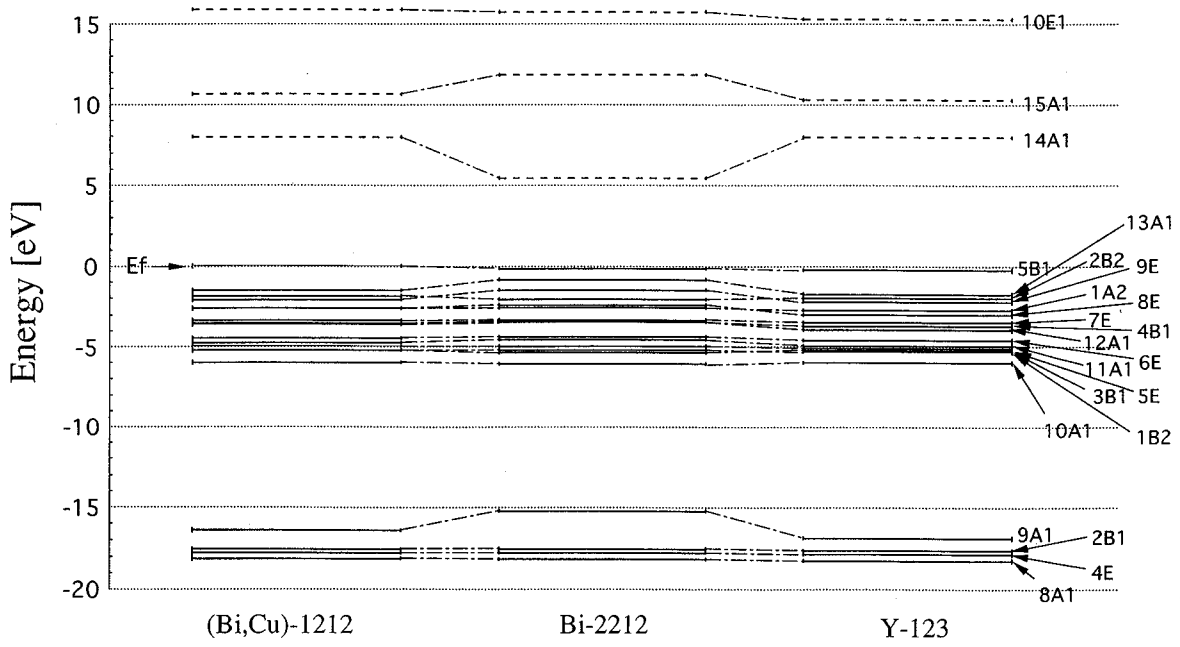

FIG. 10. Molecular orbital energy levels near Fermi level (E_f) calculated by the DV-$X\alpha$ method.

numbers thus obtained are listed in Table IV. The doped holes were mainly distributed to the O(plane) while a few holes were distributed to the O(apex) and Cu(plane). However, a slight difference exists in the hole distribution to the O(apex). About 10% of the doped hole is distributed to the O(apex) site for the (Bi,Cu)-1212 and Bi-2212 phases, while about 20% of the doped holes are distributed to that for the Y-123 phase. In order to make clear the cause for the hole distribution to the O(apex) of the Y-123 to be twice as large as that for (Bi,Cu)-1212 or Bi-2212, the parameters of the Cu-O(plane) length, Cu-O(apex) length, and buckling were varied independently. As a result, a decrease in the Cu-O(apex) length was found to be the most effective for an increase in the hole at the O(apex) site. Increasing both the Cu-O(plane) length and buckling of the O-Cu-O(plane) were less effective for the increase in the hole at the O(apex) site.

From the DV-$X\alpha$ calculation, it is found that if a hole is doped to the CuO_5 cluster, the holes will be located at the Cu-O(plane) orbital, resulting in the (Bi,Cu)-1212 phase showing a metallic property. Considering that the hole density measured by the Hall effect is much smaller than that calculated by the Mott-Hubbard model as described above, it is suggested that a hole is not doped to the CuO_5 cluster but localized in the $(Bi,Cu)O_z$ block layer. Thus, the origin of nonsuperconductivity of (Bi,Cu)-1212 is found to be localization of holes in the block layer. It is promising to substitute the blocking layer for another element to inhibit the localization of holes in the $(Bi,Cu)O_z$ block layer.

TABLE IV. The doped hole distribution on each element.

	(Bi,Cu)-1212	Bi-2212	Y-123
Cu(plane)	−0.393	−0.51	−0.415
O(apex)	0.019	0.016	0.031
O(plane) (×4)	0.133	0.164	0.136
Total	0.16	0.16	0.16
O (apex)/total	11.8%	10.0%	19.4%

B. $[M_{0.33}Cu_{0.67}]Sr_2YCu_2O_y$

As described above, it was found that $[Bi_{0.33}Cu_{0.67}]Sr_2YCu_2O_y$ does not exhibit superconductivity because of the localization of holes in the block layer. So, we tried to make the $[Bi_{0.33}Cu_{0.67}]Sr_2YCu_2O_y$ superconducting by substitution of Bi for the other elements. We examined various metal elements for the substitution of Bi. We referred to the compounds of $(M_xCu_{1-x})Sr_2YCu_2O_y$ (Refs. 14 and 15) to choose the most promising element (M = Li, Co, Ni, Zn, Ph, Al, Ga, In, As, Cr, Fe, Ge, Sn, Se, Ti, Zr, Ru, Pt, V, Nb, Ta, Mo, W, Re, and Os).

When the element, M was Co, Al, Ga, Fe, Ti, Cr, Ge, V, Mo, W, and Re, a single phase of 1212 phase was formed. Among these single-phase compounds, that with M = Mo exhibited superconductivity above 30 K as shown in Fig. 11.

C. $[(Bi_{1-x}Mo_x)_{0.33}Cu_{0.67}]Sr_2YCu_2O_y$

From the result of Sec. IV B, a solid solution between the (Bi,Cu)-1212 phase and the (Mo,Cu)-1212 phase appears to be suitable for inducing superconductivity. Therefore, we ex-

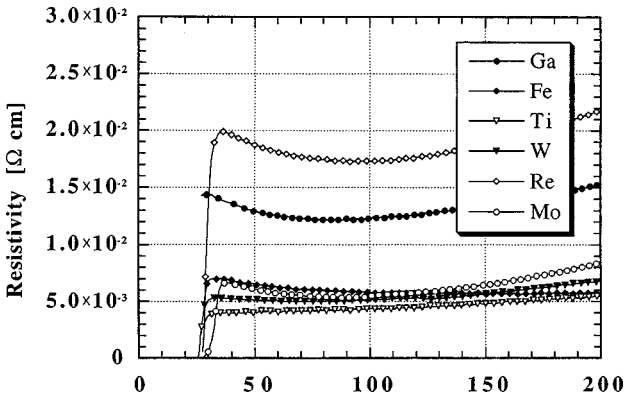

FIG. 11. Dependence of resistivity on temperature for $[M_{0.33}Cu_{0.67}]Sr_2YCu_2O_y$ (M = Ga, Fe, Ti, W, Re, and Mo).

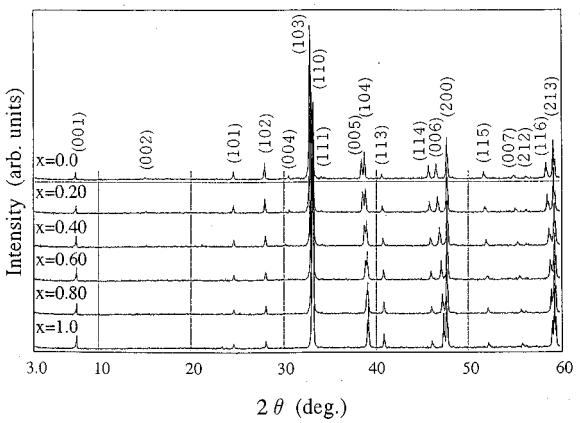

FIG. 12. XRD patterns of $[(Bi_{1-x}Mo_x)_{0.33}Cu_{0.67}]Sr_2YCu_2O_y$.

amined a range of the solid solution represented by x in $[(Bi_{1-x}Mo_x)_{0.33}Cu_{0.67}]Sr_2YCu_2O_y$. Figure 12 shows the XRD patterns for (Bi,Mo,Cu)-1212 samples prepared under various Bi/Mo ratios ($0 \leqslant x \leqslant 1.0$). In the range $0 \leqslant x \leqslant 1.0$, no peaks attributable to impurity were observed, indicating that a single phase of the (Bi,Mo,Cu)-1212 was prepared in a whole range between $(Bi_{0.33}Cu_{0.67})$-1212 and $(Mo_{0.33}Cu_{0.67})$-1212.

For the (Bi,Mo,Cu)-1212 phases, dependence of resistivity on temperature is shown in Fig. 13(a). The resistivity of a Mo-free ($x=0$) sample was so large that its resistivity was plotted with a scale of 0.1. The substitution of Mo for Bi led to a drastic decrease in resistivity. Finally, when x went up to over 0.55, a superconducting transition was observed. In Fig. 13(b), dependence of magnetic susceptibility on temperature is shown, revealing that bulk superconductivity is observed for samples with $x=0.8$ and 1.0.

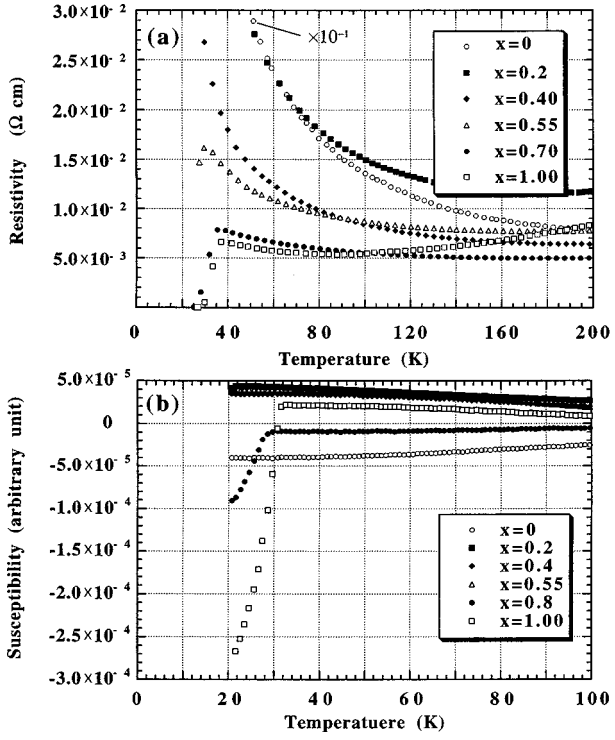

FIG. 13. Dependence of resistivity (a) and magnetic susceptibility (b) on temperature for $[(Bi_{1-x}Mo_x)_{0.33}Cu_{0.67}]Sr_2YCu_2O_y$.

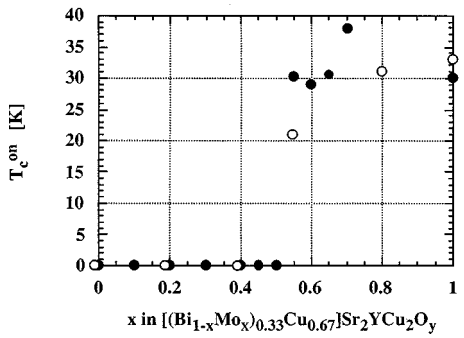

FIG. 14. T_c^{on} against composition parameter x in $[(Bi_{1-x}Mo_x)_{0.33}Cu_{0.67}]Sr_2YCu_2O_y$. ● and ○ represent T_c^{on} values measured by resistivity and magnetic susceptibility, respectively.

In order to estimate the volume fraction of the Meissner effect of the $[(Bi_{1-x}Mo_x)_{0.33}Cu_{0.67}]Sr_2YCu_2O_y$ ($x=0$) superconductor, we compared that with that of the $YBa_2Cu_3O_y$ superconductor. While the drop of the output by the Meissner effect of $YBa_2Cu_3O_y$ was -6.0×10^{-3} V/g at 22 K, that of $[(Bi_{1-x}Mo_x)_{0.33}Cu_{0.67}]Sr_2YCu_2O_y$ ($x=0$) was -2.0×10^{-3} V/g at 22 K, indicating that the volume fraction of the Meissner effect of $[(Bi_{1-x}Mo_x)_{0.33}Cu_{0.67}]Sr_2YCu_2O_y$ ($x=0$) was as large as one-third of that of the $YBa_2Cu_3O_y$ at 22 K. Even if the volume fraction of the Meissner effect of $YBa_2Cu_3O_y$ is as low as 30% at 22 K, which is considered to be the lowest estimation for the $YBa_2Cu_3O_y$ superconductor, that of the $[(Bi_{1-x}Mo_x)_{0.33}Cu_{0.67}]Sr_2YCu_2O_y$ ($x=0$) is estimated to be larger than 10%. Therefore, the $[(Bi_{1-x}Mo_x)_{0.33}Cu_{0.67}]Sr_2YCu_2O_y$ is found to be a bulk superconductor.

A correlation between the substitution ratio x and transition temperature (T_c^{on}) is shown in Fig. 14. Superconductiv-

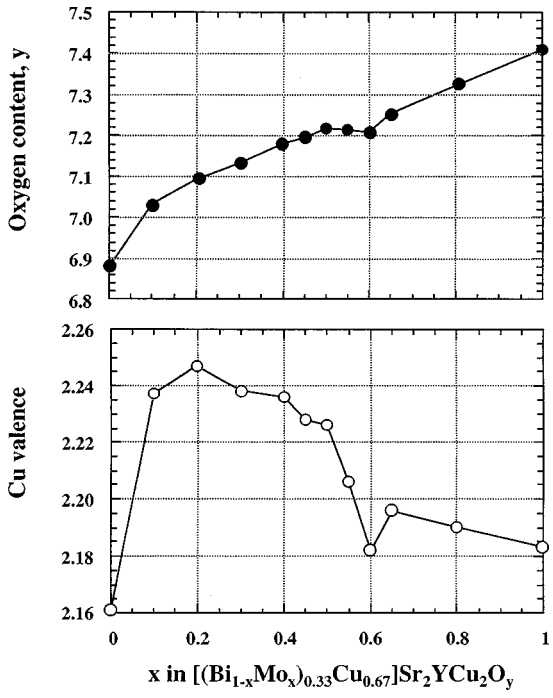

FIG. 15. Oxygen content (y) and Cu valence against Mo content x in $[(Bi_{1-x}Mo_x)_{0.33}Cu_{0.67}]Sr_2YCu_2O_y$.

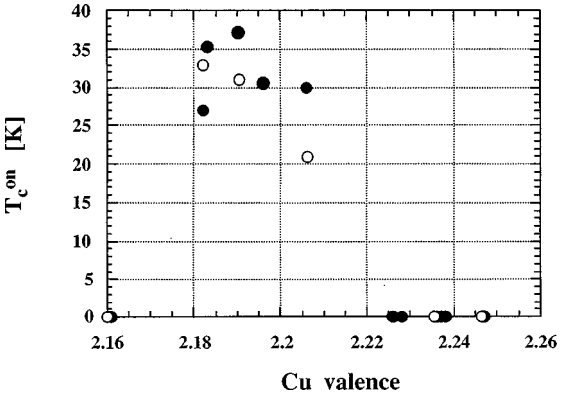

FIG. 16. T_c^{on} against Cu valence of the (Bi,Mo,Cu)-1212 phase. ● and ○ represent T_c^{on} values measured by resistivity and magnetic susceptibility, respectively.

ity is observed for the sample with $0.55 \leqslant x \leqslant 1.0$. In particular, for the samples with $x = 0.55-1.0$, the maximum T_c^{on} above 30 K was attained.

In order to clarify whether or not the Mo substitution delocalizes holes in the block layer, oxygen contents and Cu valences of the $[(Bi_{1-x}Mo_x)_{0.33}Cu_{0.67}]Sr_2YCu_2O_y$ samples were measured. As shown in Fig. 15, the oxygen content y was increased with an increase in x, although there was a slight drop for the sample with $x = 0.6$. On the other hand, the Cu valence once increased with an increase in x from 0 to 0.2 in the $[(Bi_{1-x}Mo_x)_{0.33}Cu_{0.67}]Sr_2YCu_2O_y$. However, a further increase in x above 0.2 led to a decrease in the Cu valence. Here, the valences of Bi and Mo are assumed to be Bi(III) and Mo(VI), respectively. In Fig. 16, the values of T_c^{on} were plotted against the Cu valence, showing that the maximum T_c^{on} of 37 K is obtained for the sample with a Cu valence of 2.19. Since the whole curve appears to be bell shaped as was frequently observed in high-T_c superconductors,[6,16–18] the samples, whose Cu valence is over 2.21, should be overdoped and metallic. Nevertheless, the electronic property of such samples was not metallic but semiconducting, suggesting that the samples are in the underdoped region. Therefore, it is difficult to explain the change in T_c simply by a change in the Cu valence.

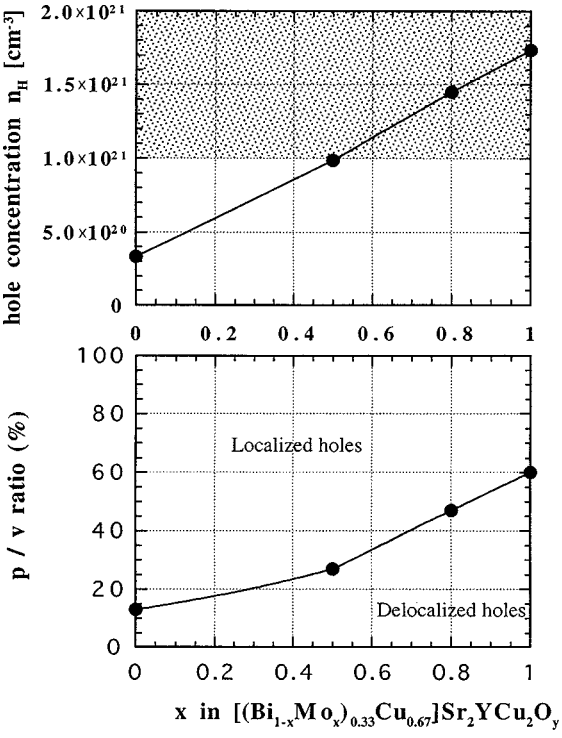

FIG. 17. Hole concentration (n_H) and p/v ratio against Mo content x in $[(Bi_{1-x}Mo_x)_{0.33}Cu_{0.67}]Sr_2YCu_2O_y$.

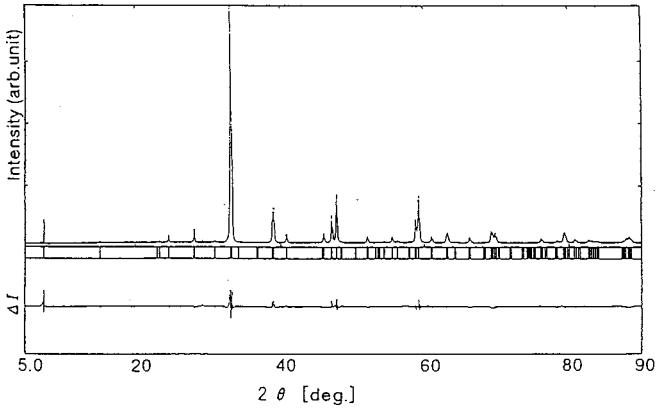

FIG. 18. An XRD pattern of $[(Bi_{0.45}Mo_{0.55})_{0.33}Cu_{0.67}]Sr_2YCu_2O_y$. The dotted and solid lines represent observed and calculated patterns, respectively. A pattern at the bottom is difference between the observed and calculated intensities at the same angle.

We measured hole density (n_H) at room temperature from the Hall coefficient. As shown in Fig. 17, with an increase in Mo substitution, x led to an increase in the hole density (n_H). Superconductivity occurs when n_H exceeds $1.0 \times 10^{21}/cm^3$. Based on the Mott-Hubbard theory, it has been believed that an increase in the hole density leads to an increase in the Cu valence. For the $[(Bi_{1-x}Mo_x)_{0.33}Cu_{0.67}]Sr_2YCu_2O_y$ phase, however, the increase in the hole density led to a decrease in the Cu valence, indicating that a Cu valence is not an appropriate barometer for estimating its hole density.

For the purpose of investigating the cause of the behavior against the Mott-Hubbard theory, Rietveld analysis[8] was carried out for all the (Bi,Mo,Cu)-1212 samples. For example, a

TABLE V. Crystallographic data for $[(Bi_{1-x}Mo_x)_{0.33}Cu_{0.67}]Sr_2YCu_2O_y$ ($x = 0.55$, $y = 7.22$). Lattice constants: $a = 3.8135(4)$ [Å], $c = 11.592(2)$ [Å]. Space group: Tetragonal $P4/mmm$ (Vol. A, No. 123), $R_{wp} = 6.81\%$, $R_P = 5.00\%$, $R_E = 6.94\%$, $R_I = 4.76\%$, $R_F = 4.00\%$.

Atom	Site	x	y	z	Occupancy	B [Å^2]
Bi	1*a*	0	0	0	0.1485	0.5
Mo	1*a*	0	0	0	0.1815	0.5
Cu(1)	1*a*	0	0	0	0.67	0.5
Sr	2*h*	1/2	1/2	0.1972	1	0.5
Y	1*d*	1/2	1/2	1/2	1	0.2
Cu(2)	2*g*	0	0	0.355(4)	1	0.5
O(1)	4*i*	0	1/2	0.375(2)	0.98	0.5
O(2)	2*g*	0	0	0.169(8)	0.90	1.5
O(3)	1*c*	1/2	1/2	0	0.41	1.5
O(4)	2 *f*	0	1/2	0	0.56	1

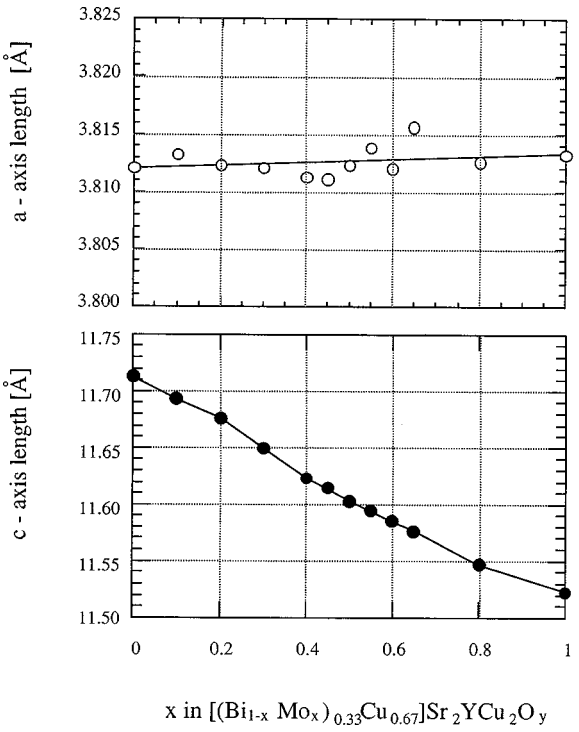

FIG. 19. Lattice constants against Mo content x in $[(Bi_{1-x}Mo_x)_{0.33}Cu_{0.67}]Sr_2YCu_2O_y$.

result of the analysis for the $x=0.55$ sample is displayed in Fig. 18 and Table V. In Fig. 18, the dotted and solid lines represent the observed and calculated XRD patterns, respectively. The pattern at the bottom of the figure shows the difference between the observed and calculated intensities at the same diffraction angle. Table V shows crystallographic data for this sample. Since the reliability factor for the analysis was $R_{wp}=6.81\%$, the proposed model appears to be an appropriate one. Its structure is composed of layers with $(Bi,Mo,Cu)O_{1+z}$, SrO, CuO_2, and Y. It is isostructural with that of the (Bi,Cu)-1212 phase (Fig. 5) except the partial substitution of Mo for Bi,Cu(1) site. From the structure refined by the Rietveld analysis, the lattice parameters of this system were plotted against the component ratio x (Fig. 19). While an a-axis length of the (Bi, Mo, Cu)-1212 phase was slightly increased with an increase in x, its c-axis length was

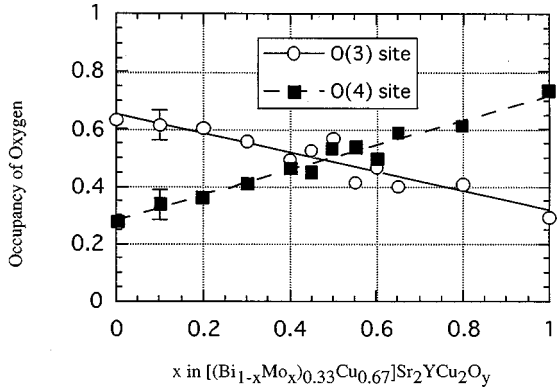

FIG. 20. Oxygen occupancy against Mo content x in $[(Bi_{1-x}Mo_x)_{0.33}Cu_{0.67}]Sr_2YCu_2O_y$. The width of the error bars show the standard deviation.

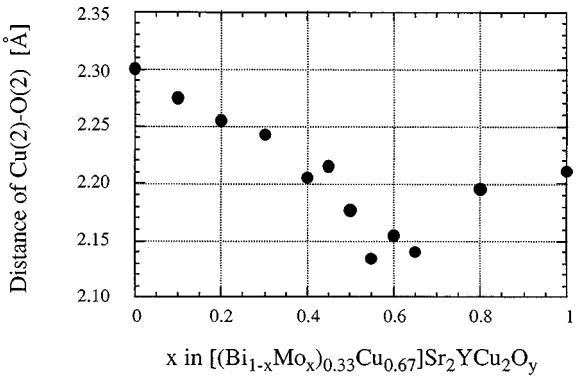

FIG. 21. Distance of Cu(2)-O(2) against Mo content x in $[(Bi_{1-x}Mo_x)_{0.33}Cu_{0.67}]Sr_2YCu_2O_y$.

decreased. However, any anomalous change in the a- and c-axis length at a value around 0.55 was not observed. On the other hand, it was found that occupancy of the oxygen sites in the block layer was remarkably changed with varying the x value. As shown in Fig. 5, there are two sorts of oxygen sites in the block layer. One is the O(3) site located in the facial center, and the other is the O(4) site located on the line between the {Bi,Mo,Cu(1)} sites. In Fig. 20, oxygen occupancies of the O(3) and O(4) sites against x in $[(Bi_{1-x}Mo_x)_{0.33}Cu_{0.67}]Sr_2YCu_2O_y$ was displayed. It is difficult to determine the oxygen site occupancy exactly from Rietveld analysis using x-ray diffraction data. However, the standard deviations of the oxygen occupancy were smaller than 10%, indicating that a systematic change in the occupancy with varying x was found. While occupancy of the O(3) site decreases with an increase in x, that of the O(4) site increases. Since the superconductivity is observed for the samples with $0.55 \leqslant x \leqslant 1.0$, the oxygen in the O(4) site with the occupancy over 0.5 may be crucial for appearance of superconductivity. Further it was found that the distance between the apical oxygen and the Cu(2) was remarkably changed. The distance between the apical oxygen O(2) and

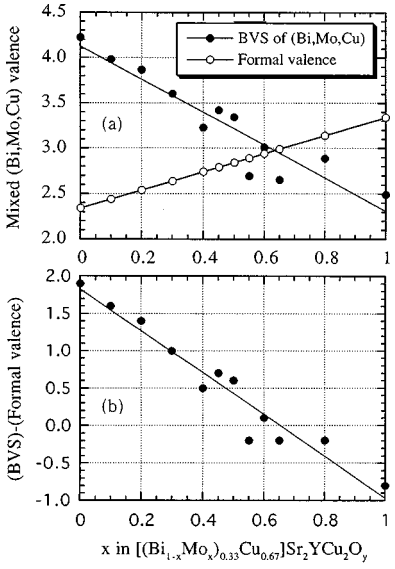

FIG. 22. BVS dependence on x in $[(Bi_{1-x}Mo_x)_{0.33}Cu_{0.67}]Sr_2YCu_2O_y$.

TABLE VI. Nonsuperconducting cuprates with a high Cu valence ($\geqslant 2.1$).

Compound	Cu valence	Electric property	Cu-O network
$BaLaRuCuO_{5.13}$	2.76	Semiconducting	CuO_6 clusters
$La_4BaCu_5O_{13}$	2.40	Metallic	3D
$(Bi_{0.33}Cu_{0.67})Sr_2YCu_2O_{6.79}$	2.36	Semiconducting	Sheets
$PrBa_2Cu_3O_y$	2.33	Semiconducting	Sheets
$La_5SrCu_6O_{15}$	2.17	Metallic	3D
$Eu_{1.5}Ba_{1.5}Cu_3O_7$	2.16	Semiconducting	Sheets

Cu(2) as a function of x is displayed in Fig. 21. While the O(2)-Cu(2) distance was decreased from 2.30 to 2.15 Å with an increase in x from 0 to 0.55, it was increased from 2.15 to 2.21 Å with a further increase in x from 0.55 to 1.0. Considering that superconductivity appears in the region of $x \geqslant 0.55$, where the Cu(2)-O(2) distance increases with the increase in x, the distance between Cu(plane) and O(apex) may be correlated with the occurrence of superconductivity.

In order to elucidate correlation between the electronic structure of the block layer and the change in the structure of the block layer, a bond valence sum (BVS) calculation was carried out.[19] In Fig. 22, the BVS of mixed (Bi,Mo,Cu) valence is plotted against the x in $[(Bi_{1-x}Mo_x)_{0.33}Cu_{0.67}]Sr_2YCu_2O_y$, clearly indicating that the BVS is drastically decreased with an increase in x. It is quite different from the formal valence drawn on the assumption that Cu, Bi, and Mo are 2+, 3+, and 6+, respectively. It is found that superconductivity occurs in the x region where the BVS is smaller than the formal valence, suggesting that Mo substitution for Bi moves localized holes to the CuO_2 layer in connection with changes in the occupancies of O(3) and O(4) in the block layer. It seems that our results are consistent with the band calculation data saying that a chemical state of the Bi is strongly affected by the structure in the block layer.[20,21] We believe that this is the origin of superconductivity for the (Bi,Mo,Cu)-1212 phase.

D. Nonsuperconducting cuprates

Various nonsuperconducting cuprates with a Cu valence over 2.1 are listed in Table VI. We have already clarified that nonsuperconductivity of $BaLaRuCuO_{5.13}$,[22] $(Bi_{0.33}Cu_{0.67})Sr_2YCu_2O_{6.79}$, and $Eu_{1.5}Ba_{1.5}Cu_3O_7$ (Ref. 23) comes from localization of holes and that the localization of holes is originated from the absence and CuO_2 sheet, the high BVS of the $(Bi_{0.33}Cu_{0.67})$ site and Cu(1) site, respectively. Further, nonsuperconductivity of $PrBa_2Cu_3O_7$ is believed to come from hybridization of the Pr_{4f} and $O_{2p\pi}$ orbitals.[24] Since these cuprates except $BaLaRuCuO_{5.13}$ have CuO_2 sheets in structure, if the trapped holes are delocalized, the cuprates will become metallic and probably superconducting.

It is well known that the treatment under high pressure oxygen has an effect on doping holes to the cuprates. By the treatment, many cuprates such as a $(La,Sr)_2CaCu_2O_y$ and $(Cu,C)Ba_2CaCu_2O_y$ induced superconductivity. We would like to emphasize that substitution of an element in the block layer also takes effect on a occurrence of superconductivity as well as the high pressure oxygen treatment. The (Bi,Mo, Cu)-1212 phase is one of the cases.

On the other hand, $La_4BaCu_5O_{13}$ and $La_5SrCu_6O_{15}$ cuprates are metallic by themselves, indicating almost all holes are originally delocalized. Accordingly, the cause of nonsuperconductivity of these cuprates are considered to be their three-dimensional Cu-O network, suggesting that the CuO_2 sheets are essential to the occurrence of superconductivity. At this stage, we are not sure how to make these metallic cuprates superconducting.

IV. CONCLUSION

A single phase of the (Bi,Cu)-1212 was successfully prepared. Two indispensable keys to prepare a single phase of (Bi,Cu)-1212 were to quench the sample after sintering, and to control x in a very narrow region around $x=0.67$ in the $(Bi_{1-x}Cu_x)Sr_2YCu_2O_y$.

From a Rietveld analysis, it was confirmed that the compound has a double CuO_2 plane. Annealing the sample in an atmosphere of oxygen led to an increase in the Cu valence as large as 2.13. However, the sample was not superconducting but semiconducting.

By combined experiments of a hole density measurement and a DV-X_α calculation, it was revealed that holes for the achievement of superconductivity were not doped to the CuO_2 plane sufficiently but were localized in the $(Bi,Cu)O_{1+z}$ plane. In order to make the (Bi,Cu)-1212 superconducting (Bi,Mo,Cu)-1212 solid solution was prepared for $0<x<1.0$ in $[(Bi_{1-x}Mo_x)_{0.33}Cu_{0.67}]Sr_2YCu_2O_y$. The samples in the region of $0.55<x<1.0$ showed superconductivity. However, the appearance of superconductivity cannot be explained only by a change in the Cu valence. Instead, it was found that the bond valence sum of the block layer was drastically changed with changes in occupancies of the oxygen sites O(3) and O(4) and the Cu(2)-O(2) distance, which may be the origin of superconductivity.

ACKNOWLEDGMENTS

We are indebted to Professor Iye of the Institute of Solid State Physics, Tokyo University for the Hall voltage measurement. We are grateful to Professor Shohno and Professor Kikuchi of IMR, Tohoku Univ. for the ICP measurement. We are thankful to Mr. Sakurai and Professor Suzuki of the Faculty of Engineering, Tohoku University for resistivity measurement, and also to Professor Maeda and Mr. Kakimoto of IMR, Tohoku University for the magnetic susceptibility measurement. Part of this work was supported by a grant from the Ministry of Education, Japan.

[1] A. Ehmann, S. Kemmler-Sack, S. Lösch, M. Shlinchenmaier, E. Wischert, P. Zoller, T. Nissel, and R. P. Huebener, Physica C **198**, 1 (1992).
[2] J. Wang, S. Takano, M. Wakata, R. Usami, K. Hamada, A. Fukuoka, and H. Yamauchi, Physica C **219**, 33 (1994).
[3] M. Wakata, S. Takano, J. Wang, A. Fukuoka, K. Isawa, and H. Yamauchi, Physica C **222**, 33 (1994).
[4] S. Kambe, T. Akao, I. Shime, S. Ohshima, and K. Okuyama, *Advances in Superconductivity VI* (Springer-Verlag, Tokyo, 1994), p. 339.
[5] S. Kambe, T. Akao, I. Shime, S. Ohshima, and K. Okuyama, Mater. Sci. Eng., B **32**, 57 (1995).
[6] S. Kambe, T. Matsuoka, M. Kawai, and M. Takahashi, Physica C **165**, 25 (1990).
[7] F. Izumi, *The Rietveld Method*, edited by R. A. Young (Oxford University Press, Oxford, 1993), Chap. 13.
[8] Y. Idemoto and K. Fueki, Physica C **168**, 167 (1990).
[9] H. Adachi, M. Tsukada, and C. Satoko, J. Phys. Soc. Jpn. **45**, 875 (1978).
[10] Z. Z. Wang, J. Clayhold, N. P. Ong, J. M. Tarascon, L. H. Greene, W. R. McKinnon, and G. W. Hull, Phys. Rev. B **36**, 7222 (1987).
[11] S. Kambe, Y. Murakoshi, R. Sekine, M. Kawai, K. Yamada, S. Ohshima, and K. Okuyama, Physica C **190**, 139 (1991).
[12] K. Imai, I. Nakai, T. Kawashima, S. Sueno, and A. Ono, Jpn. J. Appl. Phys. **27**, 1661 (1988).
[13] F. Izumi, H. Asano T. Ishigaki, E. Takayama-Muromachi, Y. Uchida, N. Watanabe, and T. Nishikawa, Jpn. J. Appl. Phys., Part 2 **26**, L649 (1987).
[14] T. Den and T. Kobayashi, Physica C **196**, 141 (1992).
[15] A. Ono, Jpn. J. Appl. Phys., Part 2 **32**, L4517 (1993).
[16] A. Maeda, M. Hase, I. Tsukada, K. Noda, S. Takebayashi, and K. Uchinokura, Phys. Rev. B **41**, 6418 (1990).
[17] T. Tamegai, N. Koga, K. Suzuki, M. Ichihara, F. Sakai, and Y. Iye, Jpn. J. Appl. Phys., Part 2 **28**, L112 (1989).
[18] A. Manthinam and J. B. Goodenough, Appl. Phys. Lett. **53**, 420 (1988).
[19] I. D. Brown and D. Aleimatt, Acta Crystallogr., Sect. B: Struct. Sci. **41**, 244 (1985).
[20] J. Ren, D. Jung, M.-H. Whangbo, J.-M. Tarascon, Y. LePage, W. R. Mckinnon, and C. C. Torardi, Physica C **158**, 501 (1989).
[21] C. C. Torardi, D. Jung, D. B. Kang, J. Ren, and M.-H. Wangbo, in *High Temperature Superconductors: Relationships Between Properties, Structure, and Solid State Chemistry*, edited by J. R. Jorgensen *et al.*, MRS Symposia Proceedings No. 156 (Materials Research Society, Pittsburgh, 1989), p. 295.
[22] S. Kambe, G. Samukawa, K. Yamaguchi, O. Ishii, I. Shime, T. Nomura, S. Ohshima, K. Okuyama, T. Itoh, H. Suematsu, and H. Yamauchi, Solid State Ionics **108**, 283 (1998).
[23] S. Ohshima, N. Tanaka, S. Kambe, and K. Okuyama, Jpn. J. Appl. Phys. **33**, 1314 (1994).
[24] R. Fehrenbacher and T. M. Rice, Phys. Rev. Lett. **70**, 3471 (1993).